

Research Paper

Delamination Fracture Analyses of Linear-Elastic Functionally Graded Beams

Victor Iliev RIZOV

*Department of Technical Mechanics
University of Architecture, Civil Engineering and Geodesy*

1 Chr. Smirnensky blvd., 1046 Sofia, Bulgaria
e-mail: V_RIZOV_FHE@UACG.BG

An analytical approach for investigation of delamination cracks in three-dimensional functionally graded linear-elastic beams was developed. Beams which are functionally graded along their width, height and length were analyzed. The fracture was studied in terms of the strain energy release rate. Beams loaded by a combination of bending moments and an axial force were considered. The approach was applied to determine the strain energy release rate for a delamination crack in a functionally graded beam of rectangular cross-section loaded in eccentric tension. An additional analysis was performed by using the beam strain energy for verification. The effects of material gradient and crack length on the delamination were evaluated.

Key words: functionally graded beam, fracture, analytical approach.

1. INTRODUCTION

Piecewise nature of laminated composites leads very often to failures from interfacial stress concentrations [1–3]. A perspective way for overcoming of this disadvantage is the concept for functionally graded materials [4]. The composition of material constituents of a functionally graded material varies continuously in structure without boundary surfaces and sudden changes of material properties. Thus, interfaces between material constituents are avoided. Besides, by spatial tailoring of material properties during manufacturing, optimum performance of functionally graded structural members and components to external loads and influences can be achieved.

Structural integrity of members and components made of functionally graded materials is strongly dependent on their fracture behaviour. Crack initiation and growth deteriorates significantly the structural capacity and functionality and may lead in some cases to catastrophic failure. That is why fracture mechanics of functionally graded materials has received considerable attention from international academic community [5–10].

Various studies on the fracture behaviour of functionally graded materials have been reviewed in [7]. Cracks oriented both parallel and perpendicular to the material gradient direction have been analyzed assuming linear-elastic behaviour of the material. Fracture of one-dimensional functionally graded materials under both static and cyclic fatigue loading conditions has been considered.

The strength of structures composed by one-dimensional functionally graded materials has been predicted by applying linear-elastic fracture mechanics [8]. Fracture behaviour of functionally graded plates under tension and beams under three-point bending has been analyzed. It has been shown that the analytical model developed yields reliable results for the strength of functionally graded structures containing re-entrant corners.

The compliance approach for analyzing fracture in one-dimensional functionally graded beam under three-point bending has been applied [9]. One equivalent homogeneous beam of variable depth for cracked functionally graded linear-elastic beam has been suggested. It has been found that the equivalent beam captures the compliance characteristics of the functionally graded beam with high accuracy. It has been concluded that the method is particularly suitable for cracked functionally graded components loaded by concentrated loads.

Yet there are crack problems which have not been analyzed sufficiently. One of these problems is the delamination fracture in three-dimensional functionally graded beams. Therefore, the main aim of present paper was to develop an analysis of delamination in beams which are functionally graded along their width, height and length. The delamination was studied in terms of the strain energy release rate by applying linear-elastic fracture mechanics.

2. ANALYSIS OF THE STRAIN ENERGY RELEASE RATE

A functionally graded beam with a delamination crack located arbitrary along the beam height (the lower and upper crack arm thicknesses are h_1 and h_2 , respectively) is under consideration in the present paper (it should be noted that the present study was motivated also by the fact that functionally graded materials can be built up layer by layer [4], which is a premise for appearance of delamination cracks between layers). The beam is under a combination of bending moments and an axial force. The beam height is $2h$. The geometry of beam cross-section is symmetric with respect to z axis. A beam portion with the crack front is shown schematically in Fig. 1. The beam width at the delamination crack level is b_s . The material of beam is functionally graded along x , y and z (the coordinate axes, x , y and z , are shown in Fig. 1). Therefore, the modulus of elasticity, E , is a function of x , y and z , i.e. $E = E(x, y, z)$.

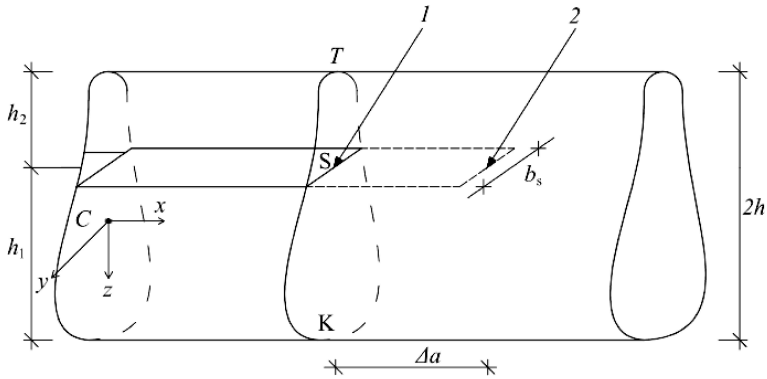


FIG. 1. A beam portion with the delamination crack front (1 – front position before the increase of crack, 2 – front position after the increase of crack).

The delamination fracture was studied in terms of the strain energy release rate. By assuming a small increase, Δa , of the crack length, the strain energy release rate, G , for linear-elastic materials can be written as [11]

$$(2.1) \quad G = \frac{\Delta U}{b_s \Delta a},$$

where the change of strain energy, ΔU , can be defined as

$$(2.2) \quad \Delta U = U_a - U_b.$$

In Eq. (2.2), U_b and U_a are the strain energies before and after the increase of crack area, respectively. The increase of crack area can be written as

$$(2.3) \quad \Delta A_a = b_s \Delta a,$$

where Δa is a small increase of the crack length.

The strain energy before the increase of crack can be calculated as

$$(2.4) \quad U_b = \iiint_{(V)} u_0 dV,$$

where

$$(2.5) \quad dV = \Delta a dA.$$

In Eq. (2.5), A is the beam cross-section area. The strain energy density, u_0 , that participates in Eq. (2.4) can be written as

$$(2.6) \quad u_0 = \frac{\sigma^2}{2E},$$

where σ is the longitudinal normal stress. The beam cross-section under a combination of bending moments, M_y and M_z , and an axial force, N , before the increase of crack is shown in Fig. 2. It was assumed that the modulus of elasticity, E , varies linearly along the width and height of beam. Besides, E varies continuously along the beam length. It was also assumed that E_T , E_L and E_K are the values of modulus of elasticity in points T , L and K (Fig. 2). The distribution of modulus of elasticity in the beam cross-section was expressed in a function of y_3 and z_3 through E_T , E_L and E_K by using the following equation [12] of a plane that passes via three points of coordinates (E_T, y_{3T}, z_{3T}) , (E_L, y_{3L}, z_{3L}) and (E_K, y_{3K}, z_{3K}) :

$$(2.7) \quad \begin{vmatrix} E & y_3 & z_3 & 1 \\ E_T & y_{3T} & z_{3T} & 1 \\ E_L & y_{3L} & z_{3L} & 1 \\ E_K & y_{3K} & z_{3K} & 1 \end{vmatrix} = 0.$$

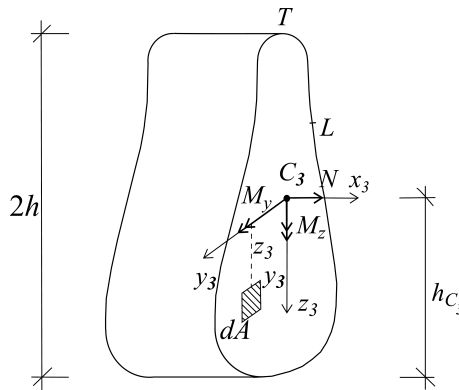


FIG. 2. Beam cross-section before the increase of crack.

It should be noted that E_T , E_L and E_K vary along the beam length, because besides along the beam height and width, the material is functionally graded also along the beam length.

The stress, σ , that is needed in order to calculate the strain energy density, u_0 , was obtained by the Hooke's law

$$(2.8) \quad \sigma = E\varepsilon,$$

where ε is the strain. The modulus of elasticity, E , is found by Eq. (2.7). It should be noted that shear stresses which arise in the delamination front area are neglected since the present study is based entirely on the classical beam theory

similarly to strain energy release rate analyses of delaminated beams performed by other authors [11, 13].

The strain, ε , was analyzed assuming validity of the Bernoulli's hypothesis for plane sections, since the span to height ratio of beams considered is large. It should be mentioned that the Bernoulli's hypothesis has been widely used when analysing fracture in functionally graded beams [8, 9]. Concerning the application of Bernoulli's hypothesis in the present study, it can also be noted that due to the fact that the beam is under a combination of bending and axial loading (Fig. 2), the only non-zero strain is the longitudinal strain, ε . Thus, according to the small strain compatibility equations, ε is distributed linearly in beam cross-section. Therefore, in the beam cross-section TLK (Fig. 2) the strain, ε , was expressed in a function of y_3 and z_3 by using the strains, ε_T , ε_L and ε_K , in points T , L and K , respectively. For this purpose, the following equation of a plane that passes through points of coordinates $(\varepsilon_T, y_{3T}, z_{3T})$, $(\varepsilon_L, y_{3L}, z_{3L})$ and $(\varepsilon_K, y_{3K}, z_{3K})$ was applied:

$$(2.9) \quad \begin{vmatrix} \varepsilon & y_3 & z_3 & 1 \\ \varepsilon_T & y_{3T} & z_{3T} & 1 \\ \varepsilon_L & y_{3L} & z_{3L} & 1 \\ \varepsilon_K & y_{3K} & z_{3K} & 1 \end{vmatrix} = 0.$$

The following equations for equilibrium of the beam cross-section (Fig. 2) were used in order to obtain the strains, ε_T , ε_L and ε_K :

$$(2.10) \quad N = \iint_{(A)} \sigma dA,$$

$$(2.11) \quad M_y = \iint_{(A)} \sigma z_3 dA,$$

$$(2.12) \quad M_z = \iint_{(A)} \sigma y_3 dA,$$

where N , M_y and M_z are the axial force and the bending moments for the y_3 and z_3 axis, respectively (Fig. 2). In Eqs. (2.10), (2.11) and (2.12) the stress, σ , is calculated by the Hooke's law, E and ε are determined by (2.7) and (2.9), respectively. The Eqs. (2.10), (2.11) and (2.12) should be solved with respect to ε_T , ε_L and ε_K for a particular form of the beam cross-section. In this way, one can determine the strain distribution in the beam cross-section before the increase of crack. Then the stress determined by (2.8) has to be substituted in (2.6) in order to obtain the strain energy density that is used to calculate U_b by (2.4).

The beam cross-section after the increase of crack is shown schematically in Fig. 3. The lower and upper crack arm heights are h_1 and h_2 , respectively. The strain energy, U_a , after the increase of crack was written as

$$(2.13) \quad U_a = U_{a_1} + U_{a_2},$$

where U_{a_1} and U_{a_2} are the strain energies in the lower and upper crack arm, respectively.

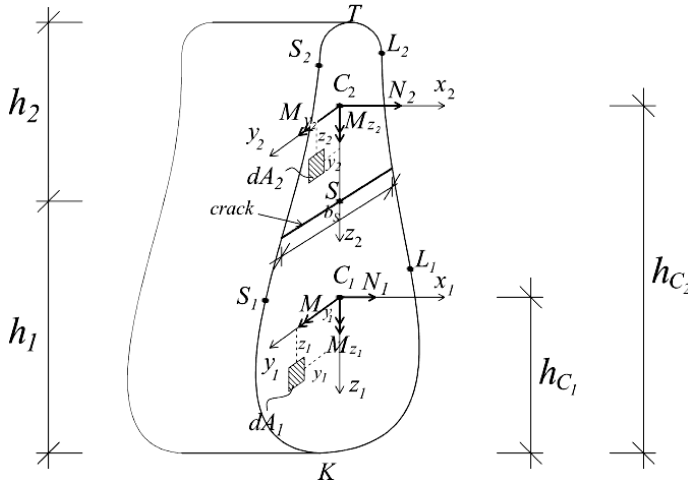


FIG. 3. Beam cross-section after the increase of crack.

The strain energy, U_{a_1} , in the lower crack arm was determined by Eq. (2.4). For this purpose, V, u_0 and dV were replaced, respectively, with V_1, u_{01} and

$$(2.14) \quad dV_1 = \Delta adA_1,$$

where u_{01} is the strain energy density in the lower crack arm, dA_1 is shown in Fig. 3 (A_1 is the area of lower crack arm cross-section). Besides, z_3 and y_3 was replaced, respectively, with z_1 and y_1 in (2.7), (2.9), (2.11) and (2.12). Also, $y_{3T}, z_{3T}, y_{3L}, z_{3L}, y_{3K}$ and z_{3K} were replaced, respectively, with $y_{1S_1}, z_{1S_1}, y_{1L_1}, z_{1L_1}, y_{1K}$ and z_{1K} in (2.7) and (2.9). In formulae (2.10), (2.11) and (2.12) the quantities N, M_y, M_z and A were replaced, respectively, with N_1, M_{y_1}, M_{z_1} and A_1 .

Formula (2.4) was used also to calculate the strain energy, U_{a_2} , in the upper crack arm after the increase of crack (Fig. 3). For this purpose, V, u_0 and dV were replaced, respectively, with V_2, u_{02} and $dV_2 = \Delta adA_2$ (u_{02} is the strain energy density in the upper crack arm). In Eqs. (2.7), (2.9), (2.11) and (2.12), the z_3 and y_3 coordinates were replaced with z_2 and y_2 , respectively. The

coordinates, y_{3T} , z_{3T} , y_{3L} , z_{3L} , y_{3K} and z_{3K} , were replaced, respectively, with y_{2S_2} , z_{2S_2} , y_{2L_2} , z_{2L_2} , y_{2T} and z_{2T} in (2.7) and (2.9). Also, N , M_y , M_z , z_3 and A were replaced, respectively, with N_2 , M_{y_2} , M_{z_2} , z_2 and A_2 in formulae (2.10), (2.11) and (2.12) (A_2 is the area of upper crack arm cross-section). Further, the cross-sectional bending moments, M_{y_2} and M_{z_2} , and the axial force, N_2 , in the upper crack arm were expressed in functions of M_y , M_z , N and M_{y_1} , M_{z_1} and N_1 by considering the equilibrium of beam cross-section (Figs. 2 and 3)

$$(2.15) \quad N_2 = N - N_1,$$

$$(2.16) \quad M_{y_2} = M_y - M_{y_1} + N(h_{C_2} - h_{C_3}) - N_1(h_{C_2} - h_{C_1}),$$

$$(2.17) \quad M_{z_2} = M - M_{z_1}.$$

Finally, by substituting of (2.2)–(2.5), (2.13) and (2.14) in (2.1), we derived

$$(2.18) \quad G = \frac{1}{b_S} \left(\iint_{(A_1)} u_{01} dA_1 + \iint_{(A_2)} u_{02} dA_2 - \iint_{(A)} u_0 dA \right).$$

3. ANALYSIS OF THE STRAIN ENERGY RELEASE RATE IN A FUNCTIONALLY GRADED BEAM LOADED IN ECCENTRIC TENSION

The analysis of strain energy release rate developed in Sec. 2 of the present paper was applied to study the strain energy release rate in the functionally graded beam shown schematically in Fig. 4. There is a delamination crack of length, a , located in the beam mid-plane. The beam is loaded by a longitudinal force, F , applied at the free end of lower crack arm (Fig. 4). Thus, the upper crack arm is free of stresses. The beam cross-section is a rectangle of width, b , and height, $2h$. The beam length is l . The material is functionally graded along the beam length, width and height. In the beam cross-section, TLK , that is located ahead of the crack front the modulus of elasticity (Fig. 5) varies according to Eq. (2.7). Along the beam length, the moduli of elasticity, E_T , E_L and E_K , vary according to the following cubic laws:

$$(3.1) \quad E_T(x) = E_{T_0} + \frac{E_{T_C} - E_{T_0}}{l^3} x^3,$$

$$(3.2) \quad E_L(x) = E_{L_0} + \frac{E_{L_C} - E_{L_0}}{l^3} x^3,$$

$$(3.3) \quad E_K(x) = E_{K_0} + \frac{E_{K_C} - E_{K_0}}{l^3} x^3,$$

where

$$(3.4) \quad 0 \leq x \leq l.$$

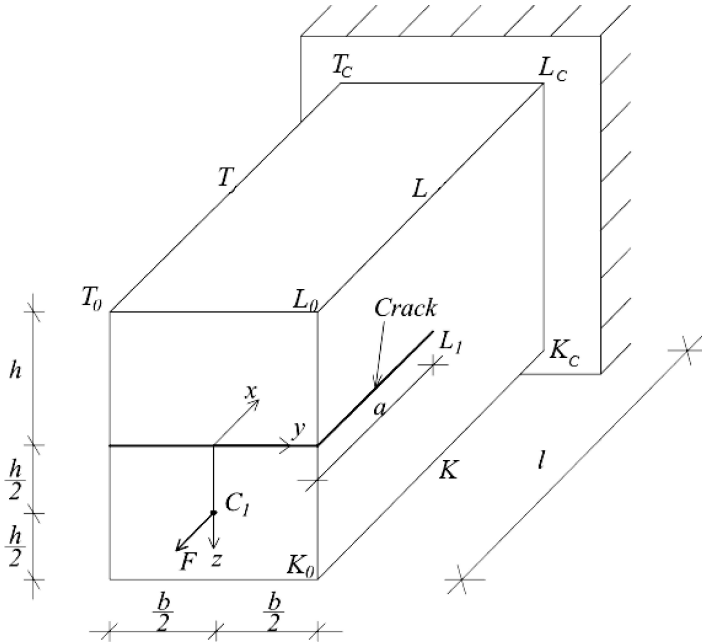


FIG. 4. A functionally graded beam configuration loaded in eccentric tension.

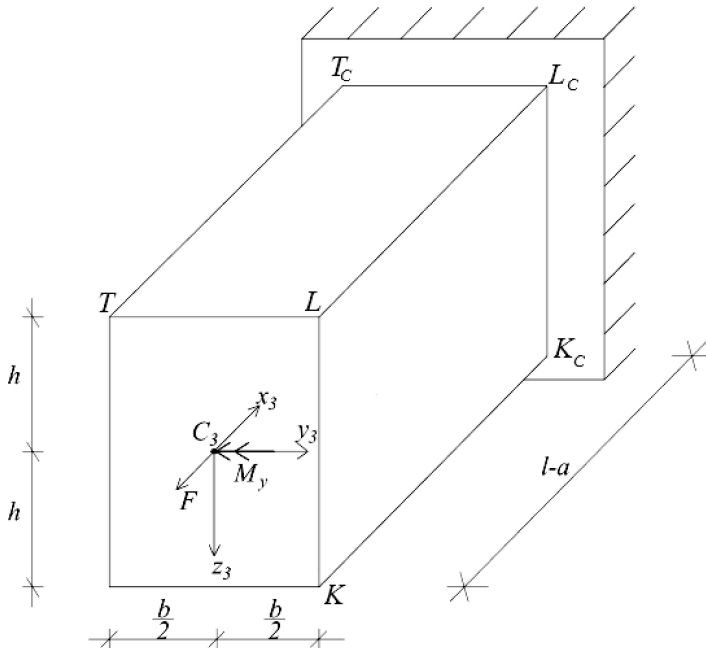


FIG. 5. The beam cross-section ahead of the crack front.

In Eqs. (3.1), (3.2) and (3.3), E_{T_0} , E_{L_0} and E_{K_0} are, respectively, the values of E_T , E_L and E_K in the free end of beam. The values of E_T , E_L and E_K in the clamped end of beam are, respectively, E_{TC} , E_{LC} and E_{KC} . The x -axis is shown in Fig. 4.

By substituting of

$$(3.5) \quad \begin{aligned} y_{3T} = -b/2, \quad z_{3T} = -h, \quad y_{3L} = b/2, \quad z_{3L} = -h, \\ y_{3K} = b/2 \quad \text{and} \quad z_{3K} = h \end{aligned}$$

in (2.7), we derived

$$(3.6) \quad E = q_1 y_3 + q_2 z_3 + q_3,$$

where

$$(3.7) \quad q_1 = \frac{1}{b} (E_L - E_T),$$

$$(3.8) \quad q_2 = \frac{1}{2h} (E_K - E_L),$$

$$(3.9) \quad q_3 = \frac{1}{2} (E_K + E_T).$$

It should be specified that in (3.7), (3.8) and (3.9), the moduli, E_T , E_L and E_K , were calculated by substituting $x = a$ in (3.1), (3.2) and (3.3).

The distribution of strains in beam cross-section, TLK , was obtained by substituting of (3.6) in (2.9)

$$(3.10) \quad \varepsilon = r_1 y_3 + r_2 z_3 + r_3,$$

where

$$(3.11) \quad r_1 = \frac{1}{b} (\varepsilon_L - \varepsilon_T),$$

$$(3.12) \quad r_2 = \frac{1}{2h} (\varepsilon_K - \varepsilon_L),$$

$$(3.13) \quad r_3 = \frac{1}{2} (\varepsilon_K + \varepsilon_T).$$

The equilibrium Eqs. (2.10), (2.11) and (2.12) were re-written for the beam cross-section ahead of the crack front (Fig. 5) as

$$(3.14) \quad N = \int_{-h}^h \left(\int_{-\frac{b}{2}}^{\frac{b}{2}} \sigma dy_3 \right) dz_3,$$

$$(3.15) \quad M_{y_3} = \int_{-h}^h \left(\int_{-\frac{b}{2}}^{\frac{b}{2}} \sigma z_3 dy_3 \right) dz_3,$$

$$(3.16) \quad M_{z_3} = \int_{-h}^h \left(\int_{-\frac{b}{2}}^{\frac{b}{2}} \sigma y_3 dy_3 \right) dz_3,$$

where (Fig. 5)

$$(3.17) \quad N = F,$$

$$(3.18) \quad M_{y_3} = F \frac{h}{2},$$

$$(3.19) \quad M_{z_3} = 0.$$

After substituting of (2.8), (3.6) and (3.10) in (3.14), (3.16) and (3.17) and solving the equations obtained with respect to r_1 , r_2 and r_3 , we derived

$$(3.20) \quad r_1 = -\frac{6q_1q_3N - 6q_1q_2M_{y_3}}{12bhq_3^3 - b^3hq_1^2q_3 - 4bh^3q_2^2q_3},$$

$$(3.21) \quad r_2 = \frac{3M_{y_3}}{2h^3bq_3} - \frac{6q_2q_3N - 6q_2^2M_{y_3}}{12hbq_3^3 - hb^3q_1^2q_3 - 4h^3bq_2^2q_3},$$

$$(3.22) \quad r_3 = \frac{6q_3N - 6q_2M_{y_3}}{12q_3^2bh - q_1^2b^3h - 4q_2^2h^3b}.$$

The distribution of strains in the beam cross-section ahead of the crack front can be obtained by substituting of (3.20), (3.21) and (3.22) in (3.10). It should be mentioned that by substituting of $E_T = E_L = E_K = E$ in (3.7)–(3.10), (3.20), (3.21) and (3.22), we derived

$$(3.23) \quad \varepsilon = \frac{F}{2bhE} + \frac{3F}{4bh^2E}z_3,$$

which is exact match of the formula [14] for strains in a homogeneous beam of cross-section, $b \times 2h$, loaded in eccentric tension by a force, F , at eccentricity, $h/2$.

The stresses distribution that is needed to obtain the strain energy density, u_0 , by (2.6) can be found by substituting of (3.6) and (3.10) in (2.8).

The cross-section, S_1L_1K , of lower crack arm behind the crack front is shown in Fig. 6. The strains distribution in cross-section, S_1L_1K , was found in the following way. First, formula (3.6) was re-written as

$$(3.24) \quad E = q_{1L}y_1 + q_{2L}z_1 + q_{3L},$$

where

$$(3.25) \quad q_{1L} = \frac{1}{b} (E_{L_1} - E_{S_1}),$$

$$(3.26) \quad q_{2L} = \frac{1}{h} (E_K - E_{L_1}),$$

$$(3.27) \quad q_{3L} = \frac{1}{2} (E_K + E_{S_1}).$$

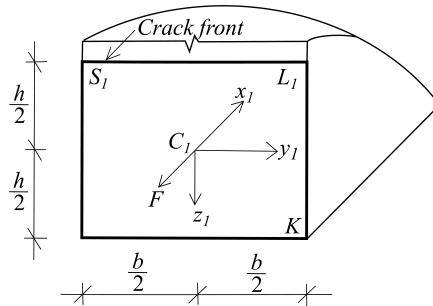


FIG. 6. The lower crack arm cross-section behind the crack front.

Axes, y_1 and z_1 , are shown in Fig. 6. In Eqs. (3.7), (3.8) and (3.9) E_{L_1} and E_{S_1} are the moduli of elasticity in points S_1 and L_1 , respectively (Fig. 6). The modulus of elasticity, E_{S_1} , was calculated by substituting $y_3 = -b/2$ and $z_3 = 0$ in (3.6). Likewise, $y_3 = b/2$ and $z_3 = 0$ were substituted in (3.6) in order to calculate the modulus of elasticity, E_{L_1} . Formula (3.10) was re-written as

$$(3.28) \quad \varepsilon = r_{1L}y_1 + r_{2L}z_1 + r_{3L},$$

where r_{1L} , r_{2L} and r_{3L} were determined by (3.20), (3.21) and (3.22), respectively. For this purpose, $M_{y_3} = 0$ was substituted in (3.20), (3.21) and (3.22). Besides, h, q_1, q_2 and q_3 were replaced with $h/2, q_{1L}, q_{2L}$ and q_{3L} , respectively. The stress that is needed to calculate the strain energy density, u_{01} , in the lower crack arm was derived by substituting of (3.24) and (3.28) in the Hooke's law (2.8).

In order to determine the strain energy release rate in the functionally graded beam configuration shown in Fig. 4, formula (2.18) was re-written as

$$(3.29) \quad G = \frac{1}{b} \left(\int_{-\frac{h}{2}}^{\frac{h}{2}} \int_{-\frac{b}{2}}^{\frac{b}{2}} u_{01} dy_1 dz_1 - \int_{-h}^h \int_{-\frac{b}{2}}^{\frac{b}{2}} u_0 dy_3 dz_3 \right).$$

In (3.29), it was taken into account that

$$(3.30) \quad b_S = b$$

for the beam under consideration (Fig. 4). Besides, $u_{02} = 0$ was substituted in (2.18), since the upper crack arm is free of stresses.

Finally, by substituting of u_0 and u_{01} in (3.29), we derived the following formula for the strain energy release rate:

$$(3.31) \quad G = \frac{1}{12} r_{1L} r_{3L} q_{1L} b^2 h + \frac{1}{12} r_{1L} r_{3L} q_{2L} h^3 + \frac{1}{24} r_{1L}^2 q_{3L} b^2 h + \frac{1}{24} r_{2L}^2 q_{3L} h^3 \\ + \frac{1}{2} r_{3L}^2 q_{3L} h - \frac{1}{6} r_1 r_{3L} q_1 b^2 h - \frac{2}{3} r_1 r_{3L} q_2 h^3 - \frac{1}{12} r_1^2 q_3 b^2 h - \frac{1}{3} r_2^2 q_3 h^3 - r_3^2 q_3 h.$$

At $E_T = E_L = E_K = E$, formula (3.30) calculates

$$(3.32) \quad G = \frac{F^2}{16Eb^2h}.$$

It should be noted that (3.32) matches exactly the formula for strain energy release rate when the beam in Fig. 4 is homogeneous [13].

An additional analysis of the strain energy release rate was performed by considering the beam strain energy in order to verify expression (3.31). For linear-elastic materials, the strain energy release rate can be derived by differentiating the strain energy, U , with respect to the crack area, A_a , [15]:

$$(3.33) \quad G = \frac{dU}{dA_a},$$

where

$$(3.34) \quad dA_a = bda.$$

In Eq. (3.34), da is an elementary increase of the crack length. By combining of (3.33) and (3.34), the strain energy release rate was written as

$$(3.35) \quad G = \frac{dU}{bda}.$$

The beam strain energy, U , was derived by integrating of the strain energy density in the lower crack arm (the strain energy in the upper crack arm is zero) and in the un-cracked beam portion

$$(3.36) \quad U = \int_{-\frac{h}{2}}^{\frac{h}{2}} \int_{-\frac{b}{2}}^{\frac{b}{2}} \int_0^a u_{01} dx dy_1 dz_1 + \int_{-h}^h \int_{-\frac{b}{2}}^{\frac{b}{2}} \int_a^l u_0 dx dy_3 dz_3.$$

The x -axis is shown in Fig. 4.

By combining of Eqs. (3.35) and (3.36), we derived formula for the strain energy release rate that is exact match of (3.31). This fact verifies the strain energy release rate analysis developed in the present paper by using the assumptions of the classical beam theory.

It should be noted that the strain energy release rate can be calculated relatively simply by (3.35) for the beam in Fig. 4. However, for more complicated structures and loading conditions, formula (2.18) has decisive advantages over (3.35). For instance, according to (2.18), the strain energy release rate can be determined by analyzing the strain energy in the beam cross-sections ahead and behind the crack front only, while formula (3.35) requires analysis of the strain energy in the whole beam structure.

The influence of material gradient on the delamination fracture behaviour of beam shown in Fig. 4 was evaluated. For this purpose, the strain energy release rate was calculated by using formula (3.31). The results obtained were presented in non-dimensional form by formula, $G_N = G/(E_{K_0}b)$. In these calculations, it was assumed that $b = 0.02$ m, $h = 0.003$ m and $F = 100$ N. The material gradient along the beam height was characterized by E_{L_0}/E_{K_0} ratio. It should be specified that E_{K_0} was kept constant. Thus, E_{L_0} was varied in order to generate various E_{L_0}/E_{K_0} ratios. The strain energy release rate was plotted in non-dimensional form against E_{L_0}/E_{K_0} ratio for three E_{T_0}/E_{K_0} ratios at $E_{K_C}/E_{K_0} = 2$, $E_{L_C}/E_{L_0} = 2$, $E_{T_C}/E_{T_0} = 2$ and $a/l = 0.5$ in Fig. 7. The curves in Fig. 7 indicate that the strain energy release rate decreases with increasing of E_{L_0}/E_{K_0} and E_{T_0}/E_{K_0} ratios. This finding was attributed to the increase of beam stiffness.

The effect of delamination crack length on the fracture behaviour was evaluated too. The delamination crack length was characterized by a/l ratio in the parametric analyses. The material gradient along the beam width was characterized by E_{T_0}/E_{L_0} ratio. The strain energy release rate was presented in non-dimensional form as a function of a/l ratio for three E_{T_0}/E_{L_0} ratios at $E_{L_0}/E_{K_0} = 0.5$, $E_{L_C}/E_{L_0} = 0.5$, $E_{T_C}/E_{T_0} = 0.5$ and $E_{K_C}/E_{K_0} = 0.5$ in Fig. 8. It can be observed in Fig. 8 that the strain energy release rate decreases with increasing of E_{T_0}/E_{L_0} ratio (this is due to the increase of beam stiffness). Con-

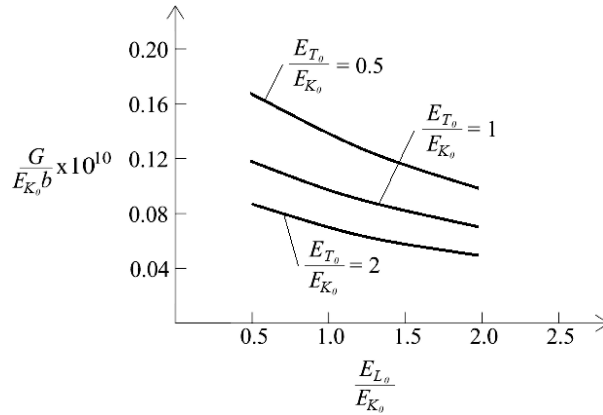


FIG. 7. The strain energy release rate in non-dimensional form plotted against E_{L_0}/E_{K_0} ratio for three E_{T_0}/E_{K_0} ratios.

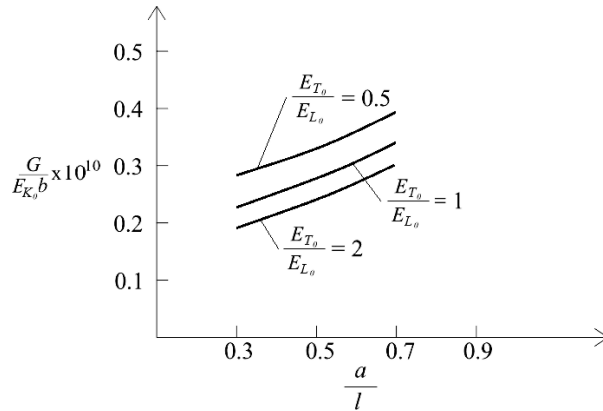


FIG. 8. The strain energy release rate in non-dimensional form presented as a function of a/l ratio for three E_{T_0}/E_{L_0} ratios.

cerning the effect of crack length, the curves in Fig. 8 indicate that the strain energy release rate increases with increasing of a/l ratio. This finding can be explained with the decrease of modulus of elasticity in the beam cross-section in which the crack front is located with increasing of the crack length, because the modulus of elasticity in the clamped end of beam is lower than in the free end of beam.

4. CONCLUSIONS

Delamination fracture in three-dimensional functionally graded beams was studied analytically. Methods of linear-elastic fracture mechanics were applied.

Fracture behaviour was studied in terms of the strain energy release rate by using the classical beam theory. Beams which are functionally graded along their width, height and length were analyzed. It was assumed that the modulus of elasticity varies linearly along the beam cross-section. The modulus of elasticity may vary arbitrary along the beam length. The delamination crack was located arbitrary along the beam height. Beams were loaded by a combination of bending moments and an axial force. The common analysis developed was applied to study the strain energy release rate for a delamination crack in a functionally graded beam configuration of a rectangular cross-section loaded in eccentric tension. In order to verify the solution derived, an additional analysis of the strain energy release rate was performed by using the beam strain energy. A parametric analysis was carried-out in order to evaluate the effects of material gradient and crack length on the fracture behaviour. It was found that the strain energy release rate decreases with increasing of E_{L_0}/E_{K_0} , E_{T_0}/E_{K_0} and E_{T_0}/E_{L_0} ratios. Also, the analysis revealed that strain energy release rate increases with increasing of crack length when the modulus of elasticity in beam clamped end is lower than in the beam free end. It should be mentioned that the analysis developed in the present paper can be applied to study the strain energy release rate in delaminated beam configurations loaded by bending moments and axial forces, such as the double cantilever beam loaded with uneven bending moments, the crack lap shear beam and others.

ACKNOWLEDGMENT

The present study was supported financially by the Research and Design Centre (CNIP) of the UACEG, Sofia (Contract BN – 189/2016).

REFERENCES

1. SZEKRENYES A., *Semi-layerwise analysis of laminated plates with nonsingular delamination -The theorem of autocontinuity*, Applied Mathematical Modelling, **40**(2): 1344–1371, 2016.
2. SZEKRENYES A., *Nonsingular crack modelling in orthotropic plates by four equivalent single layers*, European Journal of Mechanics – A/Solids, **55**(2): 73–99, 2016.
3. TKACHEVA L.A., *Unsteady crack propagation in the beam approximation*, Applied Mechanics and Technical Physics, **49**(4): 177–189, 2008.
4. BOHIDAR S.K., SHARMA R., MISHRA P.R., *Functionally graded materials: A critical review*, International Journal of Research, **1**(4): 289–301, 2014.
5. ERDOGAN F., *Fracture mechanics of functionally graded materials*, Comp. Eng., **5**(2): 753–770, 1995.
6. PAULINO G.C., *Fracture in functionally graded materials*, Engng. Fract. Mech., **69**(3): 1519–1530, 2002.

7. TILBROOK M.T., MOON R.J., HOFFMAN M., *Crack propagation in graded composites*, Composite Science and Technology, **65**(1): 201–220, 2005.
8. CARPINTERI A., PUGNO N., *Cracks in re-entrant corners in functionally graded materials*, Engineering Fracture Mechanics, **73**(1): 1279–1291, 2006.
9. UPADHYAY A.K., SIMHA K.R.Y., *Equivalent homogeneous variable depth beams for cracked FGM beams; compliance approach*, Int. J. Fract., **144**(4): 209–213, 2007.
10. SHI-DONG PAN, JI-CAI FENG, ZHEN-GONG ZHOU, WU-LIN-ZHI, *Four parallel non-symmetric Mode – III cracks with different lengths in a functionally graded material plane*, Strength, Fracture and Complexity: an International Journal, **5**(3): 143–166, 2009.
11. HSUEH C.H., TUAN W.H., WEI W.C.J., *Analyses of steady-state interface fracture of elastic multilayered beams under four-point bending*, Scripta Materialia, **60**(2): 721–724, 2009.
12. KORN G., KORN T., *Mathematical handbook for scientists and engineers* [in Russian], Nauka, Moscow, 1970.
13. HUTCHINSON J.W., SUO Z., *Mixed mode cracking in layered materials*, Advances in Applied Mechanics, **64**(2): 804–810, 1992.
14. DOWLING N., *Mechanical Behavior of Materials*, Pearson, 2007.
15. PARTON V.Z., *Fracture mechanics: from theory towards practice* [in Russian], Nauka, Moscow, 1990.

Received March 27, 2017; accepted version June 6, 2017.
